

Hybrid Quantum-Classical General Benders Decomposition Algorithm for Unit Commitment with Multiple Networked Microgrids

Fang Gao, Dejian Huang, Ziwei Zhao, Wei Dai*, Mingyu Yang, Feng Shuang*

Abstract—Unit commitment with multiple networked microgrids (UCMNM) is a typical mixed-integer nonlinear programming problem. It requires coordination between the local utility grid controlled by the distribution system operator and the microgrids controlled by the microgrid central controllers. Generalized Benders decomposition algorithm (GBDA) can effectively deal with the mixed integer problems, and we introduce quantum computing in this framework and propose a hybrid distributed decomposition algorithm in this work, named as hybrid quantum-classical generalized Benders decomposition algorithm (HQC-GBDA). For privacy-preserving and independent decision-making, HQC-GBDA decomposes the UCMNM problem into a master problem and a series of sub-problems. The NP-Hard master problem with discrete variables can be transformed into the quadratic unconstrained binary optimization (QUBO) problem, which can be settled by the quantum annealing algorithm. The main contributions of this work include: 1) Based on GBDA, we propose a multi-cut generalized Benders decomposition algorithm (MC-GBDA), which can reduce the number of iterations by adding the Benders feasibility cutting planes to the MP more efficiently; 2) In HQC-GBDA, we reconstruct the NP-Hard master problem into the QUBO problem, which is suitable to be solved by quantum computing and further reduce the complexity of the master problem, and thus improve the performance; 3) We use the D-WAVE quantum annealing machine to solve the QUBO problem of HQC-GBDA and find that HQC-GBDA is faster than its classical counterpart MC-GBDA when dealing with more complex UCMNM problems.

Index Terms—Quantum computing, Benders Decomposition. Unit commitment, Optimization

I. INTRODUCTION

Unit commitment (UC) is a very significant optimization problem in power system dispatching. It contains a large number of 0-1 variables and continuous variables, and belongs to mixed-integer quadratically constrained quadratic programming (MIQCQP). UC is nonconvex and NP-Hard because of the massive quantities of 0-1 variables. Unit commitment with multiple networked microgrids (UCMNM) requires coordination between local utility grid (LUG) and microgrids (MGs) composed of multiple distributed energy resources (DERs) to minimize the operation

charge of the power system. For the reason of privacy-preserving, each microgrid central controller (MGCC) usually does not want to expose sensitive information of its own MG, such as the charge parameters of DERs. However, without the information of MGs, it will be hard for the distribution system operator (DSO) to build the global model and then realize the coordination between the MGs and the LUG, which may threaten the security of the LUG [1]. Multiple MGs are physically networked at the assignment tier, but they had better not disclose their private information. The complexity of the UCMNM problem under this requirement greatly increases, making it difficult to be solved with global algorithms. Therefore, we need a decomposition and coordination algorithm to solve complex UCMNM problems.

Quantum Computing and Quantum Algorithms.

Quantum computing (QC) is a new computing paradigm with great potential by using quantum superposition and entanglement, and has shown quantum advantage in random quantum circuit sampling [2][3], Gaussian boson sampling [4][5] and combinatorial optimization [6]. Quantum computers follow the law of quantum mechanics, and the fundamental units are qubits. The information stored by n qubits is comparable to that by 2^n classical bits and the qubits can be operated in parallel. Quantum computers can reduce the computational complexity exponentially and thus greatly improve the computing power on specific problems.

At present, quantum computers are mainly divided into gate-model and annealing-based quantum computers [7][8][9]. In a gate-model quantum computer, different modules composed of quantum gates act on the qubits in sequence. Typical quantum algorithms are developed based on quantum gate circuits such as Shor's algorithm for integer factorization [10], Grover's algorithm for unstructured database search [11] and HHL algorithm for solving linear equations [12]. Annealing-based quantum computers run the annealing algorithm in a quantum way, such as getting rid of the local minimum and finding the global optimal solution through the process of quantum fluctuation. Under some conditions, quantum annealing is easier to converge to the global optimal value than classical annealing [9]. It is found that gate-model quantum computation

This work was supported by National Natural Science Foundation of China under Grant 61720106009 and Grant 61773359. *Corresponding author: W. Dai, F. Shuang.*

All authors are with School of Electrical Engineering, Guangxi University, Nanning, Guangxi 530004, China (e-mail: fgao@gxu.edu.cn; 2112391019@st.gxu.edu.cn; 1021313804@qq.com; weidai2019@163.com; 2012401008@st.gxu.edu.cn; fshuagn@gxu.edu.cn).

is equivalent to adiabatic quantum computation within the polynomial time complexity [13][14]. In the noisy intermediate scale quantum (NISQ) [15] era now, the number of available qubits is far from enough to solve practical problems, and the error rate of quantum gates determines that quantum circuits cannot be too deep, which promotes the birth of many hybrid quantum-classical algorithms, which use classical computing to process information to reduce the number of qubits and the depth of quantum circuits, such as improved HHL algorithms HIPEA [16] and HMPEA [17], variational quantum eigensolver (VQE) [18] and quantum approximate optimization algorithm (QAOA) [19]. The scale of problems solved by the quantum adiabatic algorithm is relatively larger. The quantum adiabatic algorithm is an effective optimization algorithm for fast searching solution space [20], and has shown speed advantage over classical computing methods in solving some complex combinatorial optimization problems [21], which can be transformed into a quadratic unconstrained binary optimization (QUBO) problem [22], specifically expressed as $\min X^T Q X$, where $X \in \{0,1\}^n$, $Q \in \mathbb{R}^{n \times n}$. With the help of quantum annealing machines such as D-WAVE, we can greatly enlarge the scale of QUBO problems we can deal with. At present, the D-WAVE quantum annealing machine has been used in practical scenarios such as protein structure design [23][24][25], manufacturing logistics scheduling, path planning [26] and financial portfolio optimization [27][28].

Distributed Decomposition Algorithms. The alternating direction method of multipliers (ADMM) is a representative distributed algorithm. Zhang, et al. [29] proposed a hybrid quantum distributed algorithm Q-ADMM based on ADMM and QAOA, and applied it to several typical UC problems. Q-ADMM could obtain smaller primal residuals with less iterations than classical ADMM and improve the computational performance. The generalized Benders decomposition algorithm (GBDA) [30], as an extension of the traditional Benders decomposition algorithm [31], is also suitable for solving mixed-integer programming problems. GBDA can use the decomposable structure of mixed-integer programming to handle the discrete (i.e., MP, short for master problem) and continuous variables (i.e., sub-problem) separately. It is worth noting that the MP in GBDA contains a large number of discrete variables and is still a NP-Hard problem. Moreover, the scale of the MP increases linearly with iterations, making the MP more challenging for classical solvers. The QC technique was used to select the cutting planes of the MP to accelerate the convergence of GBDA [32]. GBDA was also used to solve the mixed-integer linear programming problem [33], and the MP was transformed into an integer linear programming problem by continuous variable discretization, and then handled by the quantum solver. The algorithms mentioned above made great innovations and improved the performance of the distributed decomposition algorithms. However, there is still room to improve. Q-ADMM was a hybrid algorithm based on quantum circuits, which is limited by the number of available qubits and shallow quantum circuit depth in the NISQ era. So the scale of the problem that Q-ADMM could solve was limited, and Zhang et al. used Q-

ADMM to solve some simplified UC problems considering only system power demand constraints and generator output power constraints. The QC technology in [32] was only used in the selection strategy of the cutting planes, while the sub-problem and the MP were solved by the classical computer, meaning that the participation of the QC part was relatively low. The method of [33] was not suitable for MIQCQP problems such as UCMNM. Moreover, the increased scale of the MP led to more and more constraints, so it was necessary to introduce massive quantities of auxiliary binary variables for discretizing and reconstructing the MP in the form of QUBO.

To address the abovementioned issues in the UCMNM problem, we make use of the advantage of quantum computing in dealing with the QUBO problem and propose a hybrid quantum-classical generalized Benders decomposition algorithm (HQC-GBDA) under the GBDA framework. The rest of the paper is structured as follows: Section II formulates the UC problem. Section III introduces the quantum annealing algorithm, GBDA and HQC-GBDA. Section IV applies HQC-GBDA to different UC problems, and compares the performance with other algorithms. Section V summarizes the prospect and current limitations of the hybrid paradigm combining quantum computing and classical computing.

II. MATHEMATICAL MODEL OF THE UC PROBLEM

The UC problem is to minimize the operation charge of the power system $f(p_{i,t}, u_{i,t})$ (includes the total fuel charge and the startup/shutdown charge) by adjusting the on/off state and the output power of each unit under a series of system constraints (e.g., system power demand constraints, generator output power constraints, generator minimum on/off time constraints):

$$\min_{p,u} \sum_{i=1}^I \sum_{t=1}^T f(p_{i,t}, u_{i,t}),$$

$$f(p_{i,t}, u_{i,t}) = [a_i \cdot p_{i,t}^2 + b_i \cdot p_{i,t} + c_i] + d_i \cdot u_{i,t}, \quad (1)$$

where I and T represent the total number of units and time separations, respectively, $p_{i,t}$ and $u_{i,t}$ are decision variables. $p_{i,t}$ represents the output power of the unit i on the time separation t , and $u_{i,t} \in \{0,1\}$ represents the on/off state of the unit i on the time separation t (0 indicates that the unit is off while 1 indicates that the unit is on). a_i, b_i, c_i are the fuel charge parameters of the unit i , and d_i indicates the startup/shutdown charge of the unit i .

There are three kinds of constraints in the UC problem.:

$$A' \cdot U \leq B', \quad (2a)$$

$$A \cdot P \leq B, \quad (2b)$$

$$D \cdot U + G \cdot P \leq O. \quad (2c)$$

$U \in \{0,1\}^{I \times T}$, $P \in \mathbb{R}^{I \times T}$, $A \in \mathbb{R}^{I \times I}$, $B \in \mathbb{R}^{I \times T}$, $A' \in \mathbb{R}^{I \times I}$, $B' \in \mathbb{R}^{I \times T}$, $D \in \mathbb{R}^{\delta \times I}$, $G \in \mathbb{R}^{\delta \times I}$ and $O \in \mathbb{R}^{\delta \times T}$. U and P represent the matrix composed of variables $u_{i,t}$ and $p_{i,t}$ respectively. Constraints (2a) are associated only with binary variables $u_{i,t}$, such as generator minimum on/off time constraints. Constraint (2b) are associated only with continuous variables $p_{i,t}$, such as transmission line security constraints and system power demand constraints.

> REPLACE THIS LINE WITH YOUR MANUSCRIPT ID NUMBER (DOUBLE-CLICK HERE TO EDIT) <

Constraints (2c) include both binary and continuous variables, such as generator output power constraints.

III. HYBRID QUANTUM-CLASSICAL ALGORITHMS

GBDA can be used to deal with MINLP problems. Quantum annealing has advantages in solving combinatorial optimization problems expressed in the QUBO form. Taking advantages of GBDA and quantum annealing, we propose a hybrid quantum-classical decomposition algorithm HQC-GBDA. In the following, Subsection III.A. introduces the quantum annealing algorithm and briefly reviews how to solve the QUBO problem with the quantum annealing algorithm; Subsection III.B. introduces GBDA and multi-cut generalized Benders decomposition algorithm (MC-GBDA), and explains how they decompose the MINLP problem and coordinates the solving process; Subsection III.C. gives details of HQC-GBDA.

A. Quantum Annealing

Quantum annealing belongs to quantum adiabatic evolution [34], which finds the minimum of the user-defined problem Hamiltonian by adiabatic evolution of the initial system Hamiltonian. During this evolution, the system stays at its lowest energy state. At the end of quantum annealing, the solution of the corresponding problem Hamiltonian can be obtained by measurement.

The quantum annealing algorithm can be implemented on D-WAVE. The Hamiltonian of D-WAVE quantum annealing machine can be expressed with the Ising model:

$$H_{\text{Ising}} = -\frac{A(s)}{2} \left(\sum_i \hat{\sigma}_x^{(i)} \right) + \frac{B(s)}{2} \left(\sum_i h_i \hat{\sigma}_z^{(i)} + \sum_{i>j} k_{i,j} \hat{\sigma}_z^{(i)} \otimes \hat{\sigma}_z^{(j)} \right), \quad (3)$$

where $s \in [0,1]$ is the normalized anneal fraction, $\hat{\sigma}_x^{(i)}$ represents the Pauli-x operator acting on qubit i , and $\hat{\sigma}_z^{(i)}$ 、 $\hat{\sigma}_z^{(j)}$ represent the Pauli-z operator acting on qubits i and j respectively. h_i represents the bias of qubit i while $k_{i,j}$ represents coupling strength between qubits i and j . h_i and $k_{i,j}$ correspond to the coefficients of linear and quadratic terms in the QUBO-MP (i.e., Formula (19)), respectively. The first part in the right hand of Eq.(3) describes the initial Hamiltonian H_b , and the second part is the problem Hamiltonian H_p , whose lowest energy state is the optimal solution of the QUBO-MP. H_p consists of two parts, and the first part describes the influence of the external magnetic field on the spin of each qubit, while the second part describes the interaction between qubits.

To perform quantum annealing, we must first find the problem Hamiltonian H_p corresponding to the QUBO-MP, and then prepare the initial Hamiltonian H_b . With almost no interaction with external environment, the quantum system can evolve slowly enough from the initial Hamiltonian H_b to the problem Hamiltonian H_p :

$$H(t) = \left(1 - \frac{t}{T} \right) H_b + \frac{t}{T} H_p, \quad \frac{t}{T} \in [0,1], \quad (4)$$

where t is the timing point, and T is the whole annealing time.

The principle of the quantum annealing algorithm can be described as follows: (1) At $\frac{t}{T} = 0$, the quantum system is in the lowest energy state of the initial Hamiltonian H_b , that is, all qubits are in the superposition of $|0\rangle$ and $|1\rangle$ (i.e., $\frac{1}{\sqrt{2}}(|0\rangle + |1\rangle)$);

- (2) When the quantum annealing algorithm starts ($0 < \frac{t}{T} < 1$), the quantum system is slowly perturbed, and couplings and biases in the QUBO-MP Hamiltonian are introduced, making the qubits become entangled. Assuming the perturbation is long enough and changes slowly enough (i.e., the ideal quantum annealing process), the quantum system will remain in the lowest energy state without transitioning to the excited states;
- (3) When $\frac{t}{T} = 1$, the quantum annealing process ends.

Because the quantum system does not have energy level crossover during the whole quantum annealing process, the system is now in the lowest energy state of the problem Hamiltonian, which can be measured to give the solution of the QUBO-MP.

B. GBDA and MC-GBDA

For privacy-preserving and independent decision-making of each MG, GBDA and MC-GBDA can both use the decomposable structure of the UCMNM problem to handle discrete and continuous variables separately. The UCMNM problem is split into the upper MP decided by the DSO of the LUG and the lower sub-problem decided by the MGCC of each MG. The MP is a relaxation of the initial UCMNM problem, and is responsible for giving the on/off state (discrete variables) of each unit in the power system. The DSO will determine the on/off states under the pure binary variable constraints (2a) in the UCMNM problem. The sub-problem determines the output power (continuous variables) of the DERs in the MGs. The MGCCs deployed in different MGs tries to minimize the economic charge in the MGs under the current unit on/off states, considering the constraints (2b) and (2c) related to the continuous variables in the UCMNM problem. After receiving the information of unit on/off states from the DSO, each MGCC solves its sub-problem and uses the dual information and optimal solution to construct the Benders cutting planes, which are send to the DSO to determine the unit on/off states in the next iteration without revealing the sensitive information of the MG. By solving the MP and sub-problems iteratively and alternately, GBDA and MC-GBDA can gradually approach the optimal solution of the initial complex MIQCQP problem. The following gives the detailed introduction.

UCMNM is transformed into a series of nonlinear optimal economic programming sub-problems handled by MGCCs. Taking the n -th MG in the E -th iteration for example, the transformed sub-problem is:

$$\min \sum_{i=1}^{I_n} \sum_{t=1}^T f(p_{E,i,t}, u_{E,i,t}^*) = \sum_{i=1}^{I_n} \sum_{t=1}^T [a_i \cdot p_{E,i,t}^2 + b_i \cdot p_{E,i,t} + c_i] + \sum_{i=1}^{I_n} \sum_{t=1}^T d_i \cdot u_{E,i,t}^* \quad (5a)$$

s.t.

$$A \cdot P_n \leq B, \quad (5b)$$

> REPLACE THIS LINE WITH YOUR MANUSCRIPT ID NUMBER (DOUBLE-CLICK HERE TO EDIT) <

$$D \cdot U_n^* + G \cdot P_n \leq O. \quad (5c)$$

$U_n^* \in \{0,1\}^{I_n \times T}$, $P_n \in \mathbb{R}^{I_n \times T}$, $A \in \mathbb{R}^{I_n \times I_n}$, $B \in \mathbb{R}^{I_n \times T}$, $D \in \mathbb{R}^{\delta \times I_n}$, $G \in \mathbb{R}^{\delta \times I_n}$, $O \in \mathbb{R}^{\delta \times T}$. I_n is the number of units in the n -th MG. U_n^* and P_n represents the matrix composed of the on/off states (i.e., $u_{E,i,t}^*$) and output power (i.e., $p_{E,i,t}$) of the units in the n -th MG, respectively. The sub-problem is solved to give the optimal continuous variable solution p^{op} and Lagrange multiplier vectors corresponding to different constraints. Specifically, constraints (5b) and (5c) are, respectively, taken as system power demand (i.e., $P_t^D \leq \sum_{i=1}^I p_{E,i,t}$) and generator output power constraints (i.e., $p_{E,i,t} \leq P_i^{max} u_{E,i,t}$ & $p_{E,i,t} \geq P_i^{min} u_{E,i,t}$) without loss of generality.

There are two cases according to whether the sub-problem has a feasible solution:

Case 1: When the sub-problem (5) has a feasible solution, the objective function \bar{Z}_E is the optimal operation charge under the current unit on/off states. If $\bar{Z}_E < UB$, the UB (short for upper bound) of the objective function of the original problem is updated as $UB = \bar{Z}_E$. Then three multiplier vectors l^{op}, m^{op}, n^{op} can be obtained: l^{op} corresponds to constraints (5b); m^{op} and n^{op} correspond to the minimum and the maximum generator output power constraints (5c) respectively. The optimality cutting planes in the E -th iteration are constructed with the optimal solution and dual information of each MG:

$$\begin{aligned} \bar{Z} \geq & \sum_{i=1}^I \sum_{t=1}^T \left[(b_i - m_{E,i,t}^{op} + n_{E,i,t}^{op}) p_{E,i,t}^{op} + a_i (p_{E,i,t}^{op})^2 + c_i \right] + \sum_{t=1}^T \left[l_{E,t}^{op} \left(P_t^D - \sum_{i=1}^I p_{E,i,t}^{op} \right) \right] \\ & + \sum_{i=1}^I \sum_{t=1}^T (d_i + m_{E,i,t}^{op} P_i^{min} - n_{E,i,t}^{op} P_i^{max}) u_{E,i,t}, \end{aligned} \quad (6)$$

where $I = I_1 + \dots + I_n$, and P_t^D represents the system power demand at the time separation t . P_i^{min} and P_i^{max} represent the minimum and maximum output power of the unit i , respectively.

Case 2: When the sub-problem (5) has no feasible solution, relaxation variables S are introduced to construct the feasibility sub-problem. The objective function for the n -th MG is to minimize the sum of relaxation variables:

$$\min (\|l^1 S_n\|_1 + \|l^2 S_n\|_1) \quad (7a)$$

s.t.

$$A \cdot P_n \leq B + l^1 S_n, \quad (7b)$$

$$D \cdot U_n^* + G \cdot P_n \leq O + l^2 S_n, \quad (7c)$$

where $U_n^* \in \{0,1\}^{I_n \times T}$, $l^1 S_n \in \mathbb{R}^{I_n \times T}$ and $l^2 S_n \in \mathbb{R}^{\delta \times T}$ is the relaxation variables introduced into constraints (5b) and (5c) of the n -th MG, respectively. The relaxed feasibility sub-problem (7) is then solved to give the optimal solution $(p^{fea}, l^1 S_n, l^2 S_n)$ and Lagrange multipliers $(l^{fea}, m^{fea}, n^{fea})$, which are used to construct feasibility Benders cutting planes. The superscript *fea* indicates that these physical quantities are obtained when solving the feasibility sub-problem.

GBDA and MC-GBDA differ in the way to add the feasibility Benders cutting planes:

• GBDA feeds $u_{E,i,t}^*$ to the feasibility sub-problem (7), and the solution generates only one feasibility Benders cutting plane in the E -th iteration:

$$0 \geq \sum_{t=1}^T \left[\sum_{i=1}^I (m_{E,i,t}^{fea} (P_i^{min} u_{E,i,t}^* - p_{E,i,t}^{fea}) + n_{E,i,t}^{fea} (p_{E,i,t}^{fea} - P_i^{max} u_{E,i,t}^*)) \right] + l_{E,t}^{fea} \left(P_t^D - \sum_{i=1}^I p_{E,i,t}^{fea} \right) \quad (8)$$

The historical optimality and feasibility Benders cutting planes up to the E -th iteration are added to the MP to modify the optimization region, leading to the following mixed binary optimization MP (MBO-MP) of GBDA:

$$\begin{aligned} \min & \bar{Z} \\ \text{s.t.} & A' \cdot U \leq B', \\ 0 \geq & \sum_{t=1}^T \left[\sum_{i=1}^I (m_{E,i,t}^{fea} (P_i^{min} u_{E,i,t}^* - p_{E,i,t}^{fea}) + n_{E,i,t}^{fea} (p_{E,i,t}^{fea} - P_i^{max} u_{E,i,t}^*)) \right] + l_{E,t}^{fea} \left(P_t^D - \sum_{i=1}^I p_{E,i,t}^{fea} \right), \forall e \in [1, E] \\ \bar{Z} \geq & \sum_{i=1}^I \sum_{t=1}^T \left[(b_i - m_{E,i,t}^{op} + n_{E,i,t}^{op}) p_{E,i,t}^{op} + a_i (p_{E,i,t}^{op})^2 + c_i \right] + \sum_{t=1}^T \left[l_{E,t}^{op} \left(P_t^D - \sum_{i=1}^I p_{E,i,t}^{op} \right) \right] \\ & + \sum_{i=1}^I \sum_{t=1}^T (d_i + m_{E,i,t}^{op} P_i^{min} - n_{E,i,t}^{op} P_i^{max}) u_{E,i,t}, \forall e \in [1, E]. \end{aligned} \quad (9)$$

• MC-GBDA feeds $u_{E,i,t}^*$ to the feasibility sub-problem (7), and the solution generates T feasibility Benders cutting planes in the E -th iteration:

$$0 \geq \sum_{i=1}^I (m_{E,i,t}^{fea} (P_i^{min} u_{E,i,t}^* - p_{E,i,t}^{fea}) + n_{E,i,t}^{fea} (p_{E,i,t}^{fea} - P_i^{max} u_{E,i,t}^*)) + l_{E,t}^{fea} \left(P_t^D - \sum_{i=1}^I p_{E,i,t}^{fea} \right), \forall t \in [1, T]. \quad (10)$$

Similar to GBDA, the historical optimality cutting planes and T feasibility cutting planes (10) up to the E -th iteration are added as constraints of the MP to modify the optimization region, leading to the following MBO-MP of MC-GBDA:

$$\begin{aligned} \min & \bar{Z} \\ \text{s.t.} & A' \cdot U \leq B', \\ 0 \geq & \sum_{t=1}^I (m_{E,i,t}^{fea} (P_i^{min} u_{E,i,t}^* - p_{E,i,t}^{fea}) + n_{E,i,t}^{fea} (p_{E,i,t}^{fea} - P_i^{max} u_{E,i,t}^*)) + l_{E,t}^{fea} \left(P_t^D - \sum_{i=1}^I p_{E,i,t}^{fea} \right), \forall e \in [1, E], t \in [1, T] \\ \bar{Z} \geq & \sum_{i=1}^I \sum_{t=1}^T \left[(b_i - m_{E,i,t}^{op} + n_{E,i,t}^{op}) p_{E,i,t}^{op} + a_i (p_{E,i,t}^{op})^2 + c_i \right] + \sum_{t=1}^T \left[l_{E,t}^{op} \left(P_t^D - \sum_{i=1}^I p_{E,i,t}^{op} \right) \right] \\ & + \sum_{i=1}^I \sum_{t=1}^T (d_i + m_{E,i,t}^{op} P_i^{min} - n_{E,i,t}^{op} P_i^{max}) u_{E,i,t}, \forall e \in [1, E]. \end{aligned} \quad (11)$$

The objective function value \bar{Z}_E and discrete variable solution $\hat{u}_{E,i,t}$ are obtained by solving the MBO-MP of GBDA (9) or the MBO-MP of MC-GBDA (11). $\hat{u}_{E,i,t}$ represents the on/off state of the unit i at time separation t . If $\bar{Z}_E > LB$, the LB (short for lower bound) of the objective function of the initial UCMNM problem is updated as $LB = \bar{Z}_E$. If the UB and LB do not satisfy $UB - LB \leq \varepsilon$, $u_{E+1,i,t}^* = \hat{u}_{E,i,t}$ is fed into the sub-problem (5) for the next iteration. Otherwise, GBDA and MC-GBDA ends and outputs the optimal solution of the initial UCMNM problem.

> REPLACE THIS LINE WITH YOUR MANUSCRIPT ID NUMBER (DOUBLE-CLICK HERE TO EDIT) <

Although GBDA can solve the MINLP problem, the efficiency of adding feasibility and optimality cutting planes to the MP in each iteration is very low, which affects the solution speed. Obviously, the number of cutting planes added in the MBO-MP of GBDA increases linearly with iterations, and the solution will be more and more time-consuming. For example, GBDA often takes more than 12 hours to solve complex MIQCQP problems.

MC-GBDA can obtain enough feasibility cutting planes in less iterations to ensure a feasible solution of the sub-problem by adding the Benders feasibility cutting planes to the MP more efficiently. GBDA and MC-GBDA pass the optimal solution and dual information obtained in each iteration to the MBO-MP in the form of Benders cutting planes, and the size of the MBO-MP increases linearly (i.e., the size of the MBO-MP in the next iteration increases by N when the MBO-MP has N variables) or approximately linearly with iterations.

C. HQC-GBDA

To make the scale of the MP increase less than linearly with iterations, we reconstruct the NP-Hard MP in MC-GBDA into the QUBO form (QUBO-MP), and extend the classical framework of GBDA to the hybrid framework (i.e., classical computing plus quantum computing) of HQC-GBDA. Compared with MC-GBDA, HQC-GBDA further reduces the scale of the MP, and the size of the QUBO-MP remains almost unchanged with iterations, except that only the feasibility cutting planes (i.e., pure binary variable constraints) requires the introduction of a small number of auxiliary binary variables to reconstruct the MP in the QUBO form. Because the QUBO model is easily transformed into the Ising model of quantum computing, we can use the quantum annealing machine to solve the QUBO-MP efficiently and quickly, which may improve the solving speed of the distributed decomposition algorithm HQC-GBDA.

Specifically, auxiliary binary variables are introduced to transform the inequality constraints of the MBO-MP into equality constraints, which can be added as penalty terms into the QUBO matrix. The first constraint in Formula (11) is usually generator minimum on/off time constraints:

$$\sum_{j=t-T_i^{on}}^{t-1} u_{E,i,j} \geq T_i^{on} u_{E,i,t-l} (1 - u_{E,i,t-l}), \quad (12a)$$

$$\sum_{j=t-T_i^{off}}^{t-1} (1 - u_{E,i,j}) \geq T_i^{off} u_{E,i,t-l} (1 - u_{E,i,t-l}), \quad \forall t > l, \quad (12b)$$

where T_i^{on} and T_i^{off} are, respectively, the minimum on and off time of unit i . Inequality constraints (12a) and (12b) can be transformed into equality ones by introducing K_{on} and K_{off}

auxiliary binary variables respectively, where

$$K_{on} = \log_2 \left[\max \left(\sum_{j=t-T_i^{on}}^{t-1} u_{E,i,j} - T_i^{on} u_{E,i,t-l} (1 - u_{E,i,t-l}) \right) \right] \quad \text{and}$$

$K_{off} = \log_2 \left[\max \left(\sum_{j=t-T_i^{off}}^{t-1} (1 - u_{E,i,j}) - T_i^{off} u_{E,i,t-l} (1 - u_{E,i,t-l}) \right) \right]$. Finally, the corresponding QUBO matrix can be constructed by introducing

penalty coefficients ξ_{on} and ξ_{off} :

$$\xi_{on} \left(T_i^{on} u_{E,i,t-l} (1 - u_{E,i,t-l}) - \sum_{j=t-T_i^{on}}^{t-1} u_{E,i,j} + \sum_{k=0}^{K_{on}} 2^k b_k^{on} \right)^2, \quad (13a)$$

$$\xi_{off} \left(T_i^{off} u_{E,i,t-l} (1 - u_{E,i,t-l}) - \sum_{j=t-T_i^{off}}^{t-1} (1 - u_{E,i,j}) + \sum_{k=0}^{K_{off}} 2^k b_k^{off} \right)^2. \quad (13b)$$

Feasibility Benders cutting planes (10) is a series of inequality constraints. Taking the l -th constraint for example, it can be transformed into equality constraints by introducing K_{fea} auxiliary binary variables b^{fea} , where

$$K_{fea} = \log_2 \left[\max \left(\sum_{i=1}^I \left((n_{E,i,t}^{fea} p_i^{max} - m_{E,i,t}^{fea} p_i^{min}) u_{E,i,t} + (m_{E,i,t}^{fea} - n_{E,i,t}^{fea}) p_{E,i,t}^{fea} \right) \right) \right].$$

Then the penalty coefficient ξ_{fea} is introduced to construct the corresponding QUBO matrix:

$$\xi_{fea} \left(\sum_{i=1}^I (n_{E,i,t}^{fea} - m_{E,i,t}^{fea}) p_{E,i,t}^{fea} + (m_{E,i,t}^{fea} p_i^{min} - n_{E,i,t}^{fea} p_i^{max}) u_{E,i,t} \right)^2, \quad \forall t \in [1, T]. \quad (14)$$

Under specific unit on/off states and relaxation conditions, the optimal solutions p^{op}, p^{fea} and Lagrange multipliers l^{op}, m^{op}, n^{op} , l^{fea}, m^{fea} and n^{fea} are used as the model parameters of the QUBO-MP in HQC-GBDA. Benders optimality and feasibility cutting planes are returned back to the MP to modify the optimization region together with constraints associated only with binary variables, and the mast problem is reconstructed into the QUBO form:

$$\min H = H_{op} + H_{fea} + H_{cons} \quad (15a)$$

s.t.

$$H_{op} = \sum_{i=1}^I \sum_{t=1}^T \left[\sum_{e=1}^E (F_{e,i,t}^{op} + 2\mu (C_e^{op} - \bar{Z}_E) F_{e,i,t}^{op}) \right] u_{E,i,t} + \sum_{i=1}^I \sum_{t=1}^T \sum_{l=1}^T \eta \left(\sum_{e=1}^E F_{e,i,t}^{op} F_{e,i,t}^{op} \right) u_{E,i,t} u_{E,i,t}, \quad (15b)$$

$$H_{fea} = \xi_{fea} \sum_{e=1}^E \left(C_{e,i,t}^{fea} + \sum_{i=1}^I F_{e,i,t}^{fea} u_{E,i,t} + \sum_{k=0}^{K_{fea}} 2^k b_k^{fea} \right)^2, \quad (15c)$$

$$H_{cons} = \left[\begin{array}{c} \xi_{on} \\ \xi_{off} \end{array} \right] \left[\begin{array}{c} \left(T_i^{on} u_{E,i,t-l} (1 - u_{E,i,t-l}) - \sum_{j=t-T_i^{on}}^{t-1} u_{E,i,j} + \sum_{k=0}^{K_{on}} 2^k b_k^{on} \right)^2 \\ \left(T_i^{off} u_{E,i,t-l} (1 - u_{E,i,t-l}) - \sum_{j=t-T_i^{off}}^{t-1} (1 - u_{E,i,j}) + \sum_{k=0}^{K_{off}} 2^k b_k^{off} \right)^2 \end{array} \right], \quad (15d)$$

Where:

$$F_{e,i,t}^{op} = d_i + m_{e,i,t}^{op} p_i^{min} - n_{e,i,t}^{op} p_i^{max}, \quad (15e)$$

$$C_e^{op} = \sum_{i=1}^I \sum_{t=1}^T \left[(b_i - m_{e,i,t}^{op} + n_{e,i,t}^{op}) p_{e,i,t}^{op} + a_i (p_{e,i,t}^{op})^2 + c_i \right] + \sum_{i=1}^I \sum_{t=1}^T \left[l_{e,i,t}^{op} \left(p_i^D - \sum_{i=1}^I p_{e,i,t}^{op} \right) \right],$$

$$F_{e,i,t}^{fea} = m_{e,i,t}^{fea} p_i^{min} - n_{e,i,t}^{fea} p_i^{max}, \quad (15f)$$

$$C_{e,t}^{fea} = \sum_{i=1}^I \left((n_{e,i,t}^{fea} - m_{e,i,t}^{fea}) p_{e,i,t}^{fea} + l_{e,i,t}^{fea} \left(p_i^D - \sum_{i=1}^I p_{e,i,t}^{fea} \right) \right).$$

The QUBO-MP is solved to give new unit on/off states $\hat{u}_{E,i,t}$. The Hamiltonian in the QUBO form H takes discrete variables $u_{i,t}$ as decision variables, and consists of three different terms H_{op}, H_{fea} and H_{cons} . H_{op} corresponds to the QUBO form of the

> REPLACE THIS LINE WITH YOUR MANUSCRIPT ID NUMBER (DOUBLE-CLICK HERE TO EDIT) <

objective function of the MP in GBDA, which can be derived by making the objective function of the MP Z_E (i.e., the LB of the initial problem) gradually converge to the objective function of the sub-problem \bar{Z}_E (i.e., the UB of the initial problem), and μ and η are adjustable parameters [35]. H_{feu} corresponds to the QUBO form of Benders feasibility cutting planes (i.e., Formula (14)) while H_{cons} corresponds to the QUBO form of minimum on/off time constraints (i.e., Eq. (13)). HQC-GBDA converts the information into the coefficients of linear and quadratic terms of the QUBO-MP, that is, the numerical values of diagonal and non-diagonal elements (corresponding to linear and quadratic term coefficients) in the QUBO matrix change dynamically with iterations. Therefore, the size of the QUBO matrix does not increase linearly with iterations, and the size increases when only some auxiliary binary variables have to be introduced to add feasibility cutting planes during an iteration.

The procedures of HQC-GBDA are described in Fig. 1. Our proposed HQC-GBDA uses the quantum annealing algorithm to solve the QUBO-MP, and can give a high-quality solution to the UCMNM problem. At first, we set the random initial solution $u_{E,i,t}^*$ and UB and LB $UB = +\infty, LB = -\infty$. Then $u_{E,i,t}^*$ is fed into sub-problems, and the number of sub-problems is equal to N (i.e., the number of MGs in the power system). The sub-problems are handled by the MGCC in each MG. If the sub-problem has a feasible solution, the optimal solution p^{op} and Lagrange multipliers under the current unit on/off states $u_{i,t}^*$ will be obtained. The UB is updated when the sum of the objective functions of all the sub-problems \bar{Z}_E satisfies $\bar{Z}_E < UB$. If there is no feasible solution, relaxation variables S are introduced to construct the feasibility sub-problem, which gives the optimal solution (p^{feu}, S) and Lagrange multipliers.

The classical Gurobi 9 nonlinear solver is used to solve the sub-problems of optimal economic planning and relaxed feasibility sub-problems. The Benders optimality and feasibility cutting planes generated with the optimal solution and Lagrange multipliers are returned to the MP. The MP is reconstructed into the QUBO-MP and then solved by the quantum annealing algorithm to give the unit on/off states $\hat{u}_{E,i,t}$. Then $\hat{u}_{E,i,t}$ is fed

into the formula $Z_E = \max \left\{ C_e^{op} + \sum_{i \in I} \sum_{t \in T} F_{e,i,t}^{op} \hat{u}_{i,t} \mid e = 1, \dots, E \right\}$ to determine whether to update the LB. Here the C_e^{op} and $F_{e,i,t}^{op}$ are obtained in the QC step. HQC-GBDA ends when the difference of the UB and LB converges to the given threshold, and the converged bound is regarded as the minimized operation charge in the UCMNM problem. Otherwise, $u_{E+1,i,t}^* = \hat{u}_{E,i,t}$ is fed into the sub-problem for the next iteration, and the total number of iterations E is increased by 1.

IV. NUMERICAL RESULTS

This section illustrates the performance of HQC-GBDA in

solving different UC problems. In HQC-GBDA, the classical nonlinear solver Gurobi 9 is used to solve the sub-problem, while the D-WAVE *LeapTM* quantum solver is used to solve the QUBO-MP. In the following, a 6-Bus System and the UCMNM problem with three MGs in multiple scenarios are taken as example.

A. 6-Bus System

The first test system is a 6-bus system with three generators shown in Fig. 2. The three generators need to meet the hourly system power demand. Parameters of the three DERs and the hourly power demand profile are given in [36].

The operation charges by HQC-GBDA are compared with that by the classical solver Gurobi 9 in Table I. Fig. 3(a) and Fig.3(b) show the unit on/off states and the output power of each generator respectively when using HQC-GBDA. Fig.3(c) and Fig.3(d) compare the convergence behavior of GBDA, MC-GBDA and HQC-GBDA.

The 24-hour operation plan can be obtained from Fig.3(a)(b): Generator G1 is on from the very beginning and participate in the whole power generation process. Generator G3 participates in the power generation process from the 9-th to 23-th hour, while generator G2 does not participate in the power generation process at all. This is reasonable since the generation charge of G1 is the lowest while that of G2 is the highest. Fig. 3 (c) shows curves of the UB and LB of the objective function with different algorithms, and the algorithms end iterations when the UB and LB converge to the same value. Fig. 3(d) shows the difference between the UB and LB varies with iterations, and the algorithms converge when the difference is reduced to 0. Table I and Fig. 3 (c) (d) show that HQC-GBDA converges in about two iterations to give a high-quality feasible solution, while GBDA and MC-GBDA converge in 16 and 4 iterations respectively to give the same results as HQC-GBDA.

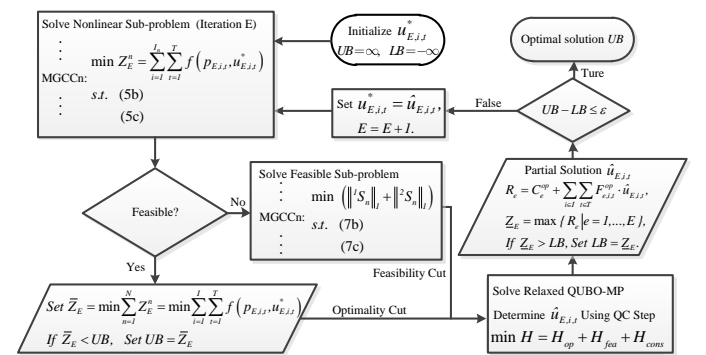


Fig. 1. The flow chart of HQC-GBDA for solving the UCMNM problem

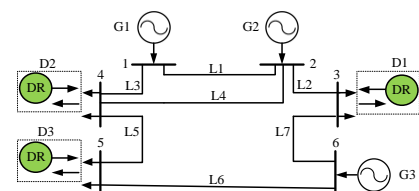


Fig. 2. Structure diagram of the 6-bus system

> REPLACE THIS LINE WITH YOUR MANUSCRIPT ID NUMBER (DOUBLE-CLICK HERE TO EDIT) <

TABLE I. Operation charges of the 6-Bus system

Unit No.	Gurobi 9	Iterations	HQC-GBDA	Iterations
G 1	\$68925.77	—	\$68925.77	—
G 2	\$3120.00	—	\$3120.00	—
G 3	\$10702.06	—	\$10702.06	—
Total	\$82747.82	129	\$82747.82	2

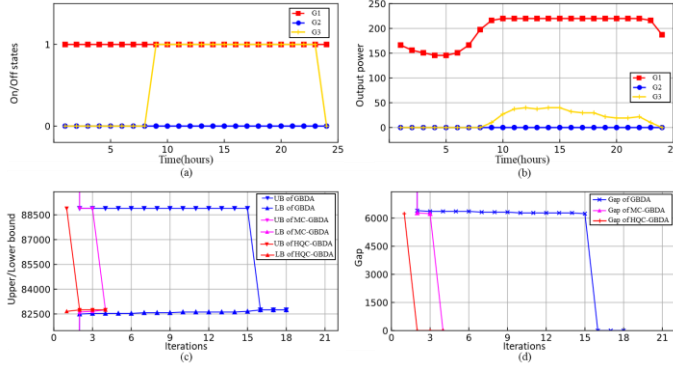


Fig. 3. (a) 24-hour unit on/off states, (b) 24-hour output power, (c) the UB and LB (d) the gap between UB and LB

B. UCMNM Problem in Different Scenarios

Cooperation between multiple networked MGs and LUG exists in the UCMNM problem. The classical nonlinear solver Gurobi 9 adopts the strategy of global modeling to solve the UCMNM problem, which means that the LUG has to know the sensitive information of each MG. Under our HQC-GBDA framework, the LUG does not need to know the sensitive information of the MGs. Fig. 4 depicts the operation mode under our HQC-GBDA framework. The local utility power grid is controlled by the DSO. The quantum annealing algorithm is employed to solve the QUBO-MP. When the quantum annealing ends, the UB of operation charge of the power system is obtained by measuring the expected value of the Ising model Hamiltonian, and the classical optimal plan (i.e., the unit on/off states in the MGs) is obtained by measuring the quantum state. After each MGCC in the MGs receives the on/off state sent by the DSO, the unit output power is obtained by solving the sub-problems of the MGs. MGCCs return the Benders cutting planes to the DSO while privacy-preserving of the MGs. HQC-GBDA converts the Benders cutting planes and generator minimum on/off time constraints into the QUBO matrix, which corresponds to the Ising model Hamiltonian and is provided to the DSO to determine the optimal commitment plan in the next iteration. In the following, HQC-GBDA is applied to the UCMNM problem in three scenarios.

Scenario 1: A small network consisting of three MGs is considered, and each MG is assigned a DER to satisfy the hourly power demand. Parameters of each DER and the hourly power demand profile are given in [36].

The operation charges by HQC-GBDA are compared with those by Gurobi 9 in Table II. Fig. 5(a) and Fig. 5(b) show the on/off state and the output power of each DER respectively when using HQC-GBDA. Fig. 5(c) and Fig. 5(d) compare the

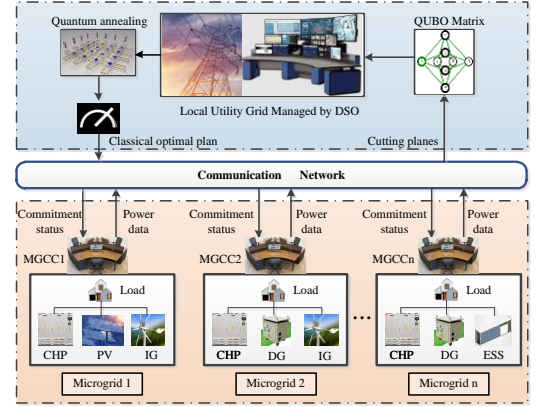


Fig. 4. Cooperative operation mode between the LUG and multiple networked MGs in HQC-GBDA

convergence behavior of GBDA, MC-GBDA and HQC-GBDA.

Fig. 5(a) and Fig. 5(b) give the 24-hour operation plan: DER1 and DER3 are in on status from the very beginning and participate in the whole power generation process; DER2 participates in the power generation process from the 7-th to the 22-th hour. This is because DER1 is the most economical while DER2 is the least economical. The same convergence analysis as the 6-bus system is performed here, and the results are shown in Fig. 5(c) and Fig. 5(d). It has to be noted that Fig. 5(c) and Fig. 5(d) are in the form of double Abscissa. The lower Abscissa represents the number of iterations of GBDA, while the upper Abscissa represents the number of iterations of HQC-GBDA and MC-GBDA. Table II, Fig. 5(c) and Fig. 5(d) show that HQC-GBDA converges in about two iterations to obtain a high-quality feasible solution, while GBDA and MC-GBDA converge in 85 and 4 iterations respectively to obtain the same results as HQC-GBDA.

Scenario 2: The same network as scenario 1 is considered. but the time planned is expanded from 24 hours to 168 hours (i.e., one week). The hourly power demand of the network is proportionally reduced by 10% every other day, as given in [36].

The operation charges with Gurobi 9 and HQC-GBDA are listed in Table III. Fig. 6(a) and Fig. 6(b) give the on/off state and the output power of each DER obtained by HQC-GBDA. The convergence behavior of MC-GBDA and HQC-GBDA is compared in Fig. 6(c) and Fig. 6(d).

Fig. 6(a) and Fig. 6(b) show the one-week operation plan: DER1 is in on status from the very beginning and participates in the whole power generation process; DER2 participates in the power generation process in the time separations 7-22, 31-46, 55-69, 79-93, 105, 106, 110-116, 129-130, 134-140, 161-162 hours; DER3 participates in the power generation process in the time separations 1-96, 99-120, 123-144, 148-168 hours. Results in Table II and Table III show that the operation charge of each MG in the second UCMNM scenario increases due to the longer operation time. Fig. 6(c) and Fig. 6(d) perform the convergence analysis. Table III and Fig. 6(c) (d) show that HQC-GBDA converges in about 3 iterations to obtain a high-

> REPLACE THIS LINE WITH YOUR MANUSCRIPT ID NUMBER (DOUBLE-CLICK HERE TO EDIT) <

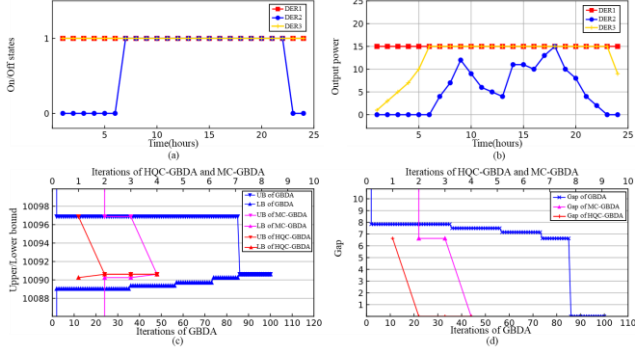


Fig. 5. (a) 24-hour unit on/off states, (b) 24-hour output power, (c) the UB and LB, and (d) gap between UB and LB in the first UCMNM scenario

TABLE II. Operation charges in the first UCMNM scenario

Unit No.	Gurobi 9	Iterations	HQC-GBDA	Iterations
MG 1	\$3282.00	—	\$3282.00	—
MG 2	\$3560.74	—	\$3560.74	—
MG 3	\$3247.88	—	\$3247.88	—
Total	\$10090.62	9	\$10090.62	2

quality solution, while MC-GBDA converges in 5 iterations to obtain the same results as HQC-GBDA. Because GBDA cannot converge to the optimal solution within 12 hours, the convergence behavior of GBDA is not shown in Fig. 6(c) (d).

Scenario 3: Each MG consists of three schedulable DERs, and the power is generated by 9 schedulable DERs cooperatively. Parameters of the 9 DERs and the hourly power demand profile are given in [36].

The operation charges in scenario 3 with Gurobi 9 and HQC-GBDA are listed in Table IV. Fig. 7(a) and Fig. 7(b) give the on/off state and the output power of each DER obtained by HQC-GBDA. The convergence behavior of GBDA, MC-GBDA and HQC-GBDA is compared in Fig. 7(c) and Fig. 7(d). Fig. 7(a) (b) show the operation plan within 24 hours: In MG 1, DER1 and DER3 are in on status from the very beginning and participate in the whole power generation process, while DER2 participates in the power generation process in the time separation 6-th to 23-th hours. In MG 2, DER4 and DER6 are in on status from the very beginning and participate in the whole power generation process, while DER5 participates in the power generation process in the time separation 6-th to 18-th hours. In MG 3, DER8 is in on status from the very beginning and participates in the whole power generation process, while DER7 and DER9 participate in the power generation process in the time separations 15-20 and 6-23 hours, respectively. Compared with scenario 1, the operation charge of each MG increases since the hourly power demand and the number of DERs in each MG increase in scenario 3. The same form of double Abscissa as in Fig. 5(c)(d) is adopted in Fig. 7(c)(d). The convergence behavior in Fig. 7(c)(d) show that HQC-GBDA converges in about 4 iterations to obtain a high-quality feasible solution, while GBDA and MC-GBDA converge in 6 and 149 iterations respectively to obtain the same results as

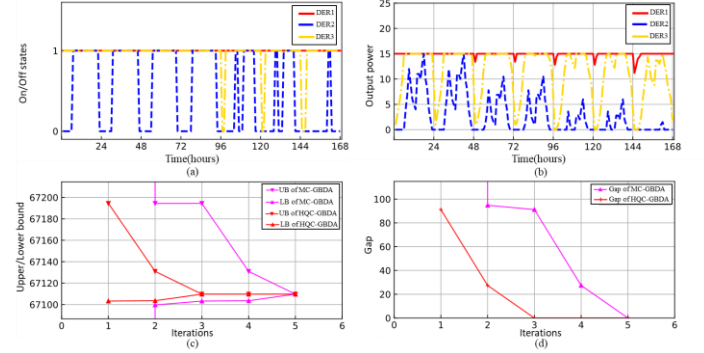


Fig. 6. (a) one-week unit on/off states, (b) one-week output power, (c) the UB and LB, and (d) gap between UB and LB in the second UCMNM scenario

TABLE III. Operation charges in the second UCMNM scenario

Unit No.	Gurobi 9	Iterations	HQC-GBDA	Iterations
MG 1	\$22926.97	—	\$22926.97	—
MG 2	\$22538.00	—	\$22538.00	—
MG 3	\$21644.75	—	\$21644.75	—
Total	\$67109.73	77	\$67109.73	3

TABLE IV. Operation charges of MGs in the UCMNM third scenario

Unit No.	Gurobi 9	Iterations	HQC-GBDA	Iterations
MG 1	\$10559.57	—	\$10568.38	—
MG 2	\$7518.21	—	\$7518.21	—
MG 3	\$8241.45	—	\$8232.49	—
Total	\$26319.23	592	\$26319.08	4

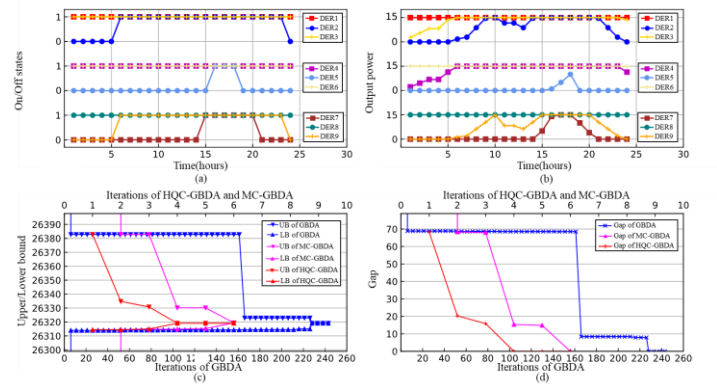


Fig. 7. (a) 24-hour unit on/off states, (b) 24-hour output power, (c) the UB and LB, and (d) gap between UB and LB in the third UCMNM scenario

HQC-GBDA.

Scenario 4: In order to further evaluate the performance of HQC-GBDA, we continue to expand the planned power generation time on the basis of scenario 1, that is, the hourly power demand everyday is the same as that in scenario 1. Fig. 8 shows the solution time with different distributed decomposition algorithms.

> REPLACE THIS LINE WITH YOUR MANUSCRIPT ID NUMBER (DOUBLE-CLICK HERE TO EDIT) <

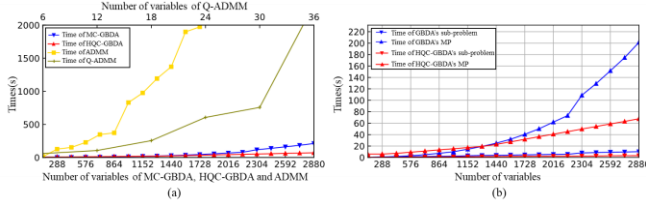


Fig. 8. The solution time of different algorithms in the fourth UCMNM scenario

TABLE V. Performance comparison in scenarios 1, 2 and 3. All times are in second.

UCMNM		Classical		Quantum
		GBDA	MC-GBDA	HQC-GBDA
3-24	Iterations	86	4	2
	Total time	14.07	0.59	6.15
	Time of MP	8.46	0.22	5.99
	Time of sub-problem	5.61	0.37	0.16
	MP scale	6192	216	80
3-168	Iterations	—	5	3
	Total time	—	16.56	16.34
	Time of MP	—	13.16	15.24
	Time of sub-problem	—	3.40	1.10
	MP scale	—	1512	583
9-24	Iterations	227	6	4
	Total time	122.64	3.99	12.77
	Time of MP	55.48	2.57	11.97
	Time of sub-problem	67.16	1.42	0.80
	MP scale	49032	1080	262

The Abscissa of Fig. 8(a) and Fig. 8(b) is the total number of discrete and continuous variables in the UCMNM problem. Fig. 8(a) is in the form of double Abscissa. The lower Abscissa represents total number of variables of MC-GBDA, HQC-GBDA and ADMM, while the upper Abscissa represents total number of variables of Q-ADMM. The Ordinates of Fig. 8(a) and Fig. 8(b) are, respectively, the time required to solve the UCMNM problem and the sub-problem/MP. It can be seen that ADMM takes more time than the algorithms in the Benders framework, which may be caused by their different frameworks. The Benders framework collects and retains the historical cutting planes generated by each sub-problem, and this strategy makes its iterations more efficient. While ADMM only relies on the exchange of information between neighboring clusters [37], making its iterations less efficient. Q-ADMM can only solve very small-scale UCMNM problems, because the Qiskit simulator we use here to construct quantum QAOA circuits in Q-ADMM can only provide a maximum number of 28 qubits. In MC-GBDA and HQC-GBDA, the sub-problems associated with continuous variables are both solved with Gurobi 9, so Fig. 8(b) shows that the solution time of the sub-problems is very small and can be ignored. The main difference lies in that the QUBO-MP in HQC-GBDA is solved with D-WAVE, which shows quantum advantage when the UCMNM problem has more than 1440 variables. This proves that HQC-GBDA is advantageous over its classic version MC-GBDA in dealing with complex UCMNM problems.

Detailed Performance Comparison: Table V shows the number of iterations, total solution time, time for the DSO to

solve MP, time for MGCCs to solve sub-problems, and the MP scale when using GBDA, MC-GBDA and HQC-GBDA to solve UCMNM problems in scenarios 1, 2 and 3. The MP scale refers to the number of variables in all the MP constraints, or the QUBO matrix dimension when the algorithms end. The two numbers in the first column in Table V indicate the number of units and time separations, respectively. It can be seen that GBDA has the most iterations, while HQC-GBDA has the least. At the end of the algorithm, the MP scale of MC-GBDA is smaller than that of GBDA, which is achieved by adding the Benders feasibility cutting planes to the MP more efficiently, making MC-GBDA have less iterations than GBDA. When the MP is reconstructed in the QUBO form in HQC-GBDA, the MP scale and thus iterations are further reduced. When the MP scale is large enough (i.e., the 3-168 UCMNM problem), the total solution time of HQC-GBDA is less than that of MC-GBDA, which is consistent with the phenomenon observed in Fig. 8.

V. CONCLUSION

For problems of unit commitment with multiple networked microgrids, the hybrid quantum-classical generalized Benders decomposition algorithm is proposed to make use of the advantage of quantum computing in solving QUBO problems. The hybrid algorithm gives the same optimal solution as the classical solver Gurobi 9 in several typical power systems. The hybrid algorithm is based on the multi-cut generalized Benders decomposition algorithm, which adopts the strategy of adding multiple feasibility cutting planes in a single iteration and thus can converge in less iterations than the original generalized Benders decomposition algorithm. The hybrid algorithm reconstructs the NP-Hard master problem in the multi-cut generalized Benders decomposition algorithm into the QUBO form, which further reduces the number of iterations required for convergence and improves the computing performance. The master problem is modelled with traditional combinational optimization schemes in classical Benders framework, while with QUBO schemes in hybrid Benders framework. Exploiting the efficiency of quantum computers in dealing with QUBO problems, the hybrid algorithm has quantum advantage in solving more complex problems. The hybrid algorithm uses the D-WAVE quantum annealing machine to solve the QUBO form of the master problem, so the solving speed will increase with the scale of the quantum annealing machine.

REFERENCES

- [1] Z. Wang, B. Chen, J. Wang, M. M. Begovic, and C. Chen, "Coordinated energy management of networked microgrids in distribution systems," *IEEE Transactions on Smart Grid*, vol. 6, no. 1, pp. 45–53, 2014.
- [2] F. Arute, K. Arya, R. Babbush, D. Bacon, J. C. Bardin, R. Barends, R. Biswas, S. Boixo, F.G.S.L. Brandao, D.A. Buell, et al., "Quantum supremacy using a programmable superconducting processor," *Nature*, vol. 574, no. 7779, pp. 505–510, 2019.
- [3] M. Gong, S. Wang, C. Zha, M. C. Chen, H. L. Huang, Y. L. Wu, Q. L. Zhu, Y. W. Zhao, S. W. Li, S. J. Guo, et al., "Quantum walks on a programmable two-dimensional 62-qubit superconducting processor," *Science*, vol. 372, no. 6545, pp. 948–952, 2021.
- [4] H. S. Zhong, H. Wang, Y. H. Deng, M. C. Chen, L. C. Peng, Y. H. Luo, J. Qin, D. Wu, X. Ding, Y. Hu, et al., "Quantum computational advantage using photons," *Science*, vol. 370, no. 6523, pp. 1460–1463, 2020.

- [5] L. S. Madsen, F. Laudenbach, M. F. Askarani, F. Rortais, T. Vincent, J. F. F. Bulmer, F. M. Miatto, L. Neuhaus, L. G. Helt, M. J. Collins, A. E. Lita, T. Gerrits, S. W. Nam, V. D. Vaidya, M. Menotti, I. Dhand, Z. Vernon, N. Quesada and J. Lavoie, "Quantum computational advantage with a programmable photonic processor," *Nature*, vol. 606, no.7912, pp.75–81, 2022.
- [6] A. Lucas, "Ising formulations of many NP problems," *Frontiers in physics*, 2014.
- [7] E. Farhi, J. Goldstone, S. Gutmann, and M. Sipser, "Quantum computation by adiabatic evolution," arXiv: 0001106, 2000.
- [8] Y. Wang, Y. Li, Z. qi Yin, and B. Zeng, "16-qubit IBM universal quantum computer can be fully entangled," *npj Quantum Information*, vol. 4, no. 1, pp. 1–6, 2018.
- [9] B. Y. E. Gibney, "Quantum computer gets design upgrade," *Nature*, vol. 541, no. 7638, pp. 447–448, 2017.
- [10] P. W. Shor, "Algorithms for quantum computation: Discrete logarithms and factoring," *Proceedings 35th annual symposium on foundations of computer science*, pp. 124–134, 1994.
- [11] L. K. Grover, "Quantum mechanics helps in searching for a needle in a haystack," *Physical Review Letters*, vol. 79, no. 2, pp. 325, 1997.
- [12] A. W. Harrow, A. Hassidim, and S. Lloyd, "Quantum algorithm for linear systems of equations," *Physical Review Letters*, vol. 103, 2009.
- [13] W. Van Dam, M. Mosca, and U. Vazirani, "How powerful is adiabatic quantum computation?" *Proceedings 42nd IEEE symposium on foundations of computer science*, IEEE, pp. 279–287, 2001.
- [14] D. Aharonov, W. V. Dam, J. Kempe, Z. Landau, S. Lloyd and O. Regev, "Adiabatic quantum computation is equivalent to standard quantum computation," *SIAM Review*, vol. 50, no. 4, pp. 755–787, 2008.
- [15] J. Preskill, "Quantum computing in the NISQ era and beyond," *Quantum*, 2018.
- [16] F. Gao, G. Wu, M. Yang, W. Cui, and F. Shuang, "A hybrid algorithm to solve linear systems of equations with limited qubit resources," *Quantum Information Processing*, vol. 21, no. 3, pp. 1–31, 2022.
- [17] F. Gao, G. Wu, S. Guo, W. Dai, and F. Shuang, "Solving DC power flow problems using quantum and hybrid algorithms," arXiv: 2201.04848, 2022.
- [18] A. Peruzzo, J. M. Clean, P. Shadbolt, M. H. Yung, X. Q. Zhou, P. J. Love, A. A. Guzik and J. L. O. Brien, "A variational eigenvalue solver on a photonic quantum processor," *Nature Communications*, vol. 5, no. 1, pp. 1–7, 2014.
- [19] E. Farhi, J. Goldstone, and S. Gutmann, "A quantum approximate optimization algorithm," arXiv: 1411.4028, 2014.
- [20] G. E. Santoro and E. Tosatti, "Optimization using quantum mechanics: Quantum annealing through adiabatic evolution," *Journal of Physics A: Mathematical and General*, vol. 39, no. 36, 2006.
- [21] C. C. McGeoch and C. Wang, "Experimental evaluation of an adiabatic quantum system for combinatorial optimization," *Proceedings of the ACM International Conference on Computing Frontiers*, pp. 1–11, 2013.
- [22] G. Kochenberger, J. K. Hao, F. Glover, M. Lewis, Z. P. Lu, H. B. Wang and Y. Wang, "The unconstrained binary quadratic programming problem: A survey," *Journal of Combinatorial Optimization*, vol. 28, no. 1, pp. 58–81, 2014.
- [23] A. Perdomo-Ortiz, N. Dickson, M. Drew-Brook, G. Rose, and A. Aspuru-Guzik, "Finding low-energy conformations of lattice protein models by quantum annealing," *Scientific Reports*, vol. 2, no.1, pp. 1–7, 2012.
- [24] 2021 D-Wave Systems Inc. (2021). Menten AI battles COVID-19 with quantum peptide therapeutics. [Online]. Available: https://www.dwavesys.com/media/kjof1cdh/dwave_menten-ai_case_story-2_v4.pdf, 2021.
- [25] V. Marx, "Biology begins to tangle with quantum computing," *Nature Methods*, vol. 18, no. 7, pp. 715–719, 2021.
- [26] 2021 D-Wave Systems Inc. (2021). DENSO: Imagining an optimized future with quantum computing. [Online]. Available: <https://www.dwavesys.com/solutions-and-products/manufacturing-logistics/>.
- [27] S. Mugel, C. Kuchkovsky, E. Sanchez, S. F. Lorenzo, J. L. Hita, E. Lizaso and R. Orus, "Dynamic portfolio optimization with real datasets using quantum processors and quantum-inspired tensor networks," *Physical Review Research*, vol. 4, no. 1, p.013006, 2022.
- [28] J. L. Hevia, G. Peterssen, and M. Piattini, "QuantumPath: A quantum software development platform," *Software: Practice and Experience*, vol. 52, no. 6, pp. 1517–1530, 2022.
- [29] N. Nikmehr, S. Member, P. Zhang, S. Member, and M. A. Bragin, "Quantum distributed unit commitment: An Application in Microgrids," *IEEE transactions on power systems*, 2022.
- [30] A. M. Geoffrion, "Generalized Benders decomposition," *Journal of Optimization Theory and Applications*, vol. 10, no. 4, pp. 237–260, 1972.
- [31] Z. C. Taskin, "Benders decomposition," *Wiley Encyclopedia of Operations Research and Management Science*. John Wiley & Sons, Malden (MA), 2010.
- [32] N. G. Paterakis, "Hybrid quantum-classical multi-cut Benders approach with a power system Application," arXiv: 2112.05643, 2021.
- [33] Z. Zhao, L. Fan and Z. Han, "Hybrid quantum Benders' decomposition for mixed-integer linear programming," 2022 IEEE Wireless Communications and Networking Conference (WCNC), pp. 2536–2540, 2022.
- [34] A. M. Childs, E. Farhi, and J. Preskill, "Robustness of adiabatic quantum computation," *Physical Review A*, vol. 65, no. 1, 2001.
- [35] A. Ajagekar, T. Humble, and F. You, "Quantum computing based hybrid solution strategies for large-scale discrete-continuous optimization problems," *Computers & Chemical Engineering*, vol. 132, 2020.
- [36] (2022, July 15). Unit-Commitment.github.io. [Online]. Available: <https://github.com/hdj97/Unit-Commitment.github.io>
- [37] S. Candas, K. Zhang, T. A. Hamacher, "Comparative study of benders decomposition and ADMM for decentralized optimal power flow," 2020 IEEE Power & Energy Society Innovative Smart Grid Technologies Conference (ISGT), 2020.